Numerical Study of the Thermal Behaviour of a Thermo-Structural Aeronautical Composite under Fire Stress

N Grange, K Chetehouna, Nicolas Gascoin, S Senave

▶ To cite this version:

Numerical Study of the Thermal Behaviour of a Thermo-Structural Aeronautical Composite under Fire Stress

N.GRANGE [*,1], K. CHETEHOUNA[1], N. GASCOIN [1], S. SENAVE [2]

[1]INSA Centre Val de Loire, 88 Boulevard Lahitolle, 18000 Bourges FRANCE
[2]DAHER, 23 route de Tours, 41400 St Julien de Chédon FRANCE

Abstract
The use of composite materials for aeronautical applications has been growing since several years because of the opportunity to produce lightweight structures reducing the fuel bills and emissions. The need for fireproof certification imposes costly and time consuming experiments that might be replaced or complemented in the years to come by numerical calculations. The present work creates a CFD numerical model of a fireproof test. As an example, a composite part (plenum) located in an aircraft APU (auxiliary power unit) which provides power to the aircraft is investigated. A numerical calibration of the flame is conducted according to the fireproof standards. The results of fireproof tests demonstrate a good evaluation of the plenum temperature (discrepancies lower than 19%). The influence of an internal air jet within the studied part is also evaluated ~~observed to evaluate how this could lower the requirements of certification rules.~~ A thermal decrease as high as 38 % is found for a velocity of 10 m/s.

[*] Corresponding author: nathan.grange@insa-cvl.fr

1. Introduction

The use of composite materials for aeronautical applications has been growing since several years because of the opportunity to produce lightweight structures reducing the fuel bills and emissions. The growing use of these materials leads to technical and design challenges to comply with safety standards and certifications, especially when fire safety requirements are concerned. Aircraft parts dedicated to firewall applications or located in a designated fire zone, should meet a fireproof requirement. Therefore the composite parts have to pass fire tests according to ISO 2685 [1] or FAA - AC20-135 (FAR-25) [2] standards. Both standards use an oil burner to heat the part with a minimum temperature of 1100°C for 15 minutes. In this work, a 3D numerical model of a fireproof test using a CFD code is created to investigate the predictivity of a numerical fireproof test. This numerical step is expected to replace experimentation during the development phases of the composite part before the certification test to reduce development cost. This numerical tool would help designers to choose between different composite materials and designs options to avoid critical temperature increases at certain areas and perforation in this composite part during fireproof tests. The second section is dedicated to the presentation of the experimental setup and the third one will present the physical and numerical modelling approaches. In the fourth section the computed temperatures are compared to the experimental ones to validate the presented numerical approach and the results are discussed. The influence of an internal air jet within the studied part is also evaluated ~~The feasibility of replacing a thermal protection by an internal air jet is also presented~~ in this paper as a first design variable ~~case~~.

2. Experimental setup

To be labelled "fireproof" ~~as it is requested in most of the APU (Auxiliary power unit) part specifications and~~ according to the related standards, the concerned part (here a composite plenum) has to resist 15 minutes to a calibrated flame. Criteria to establish the test is passed include no burn through of the part structure, as well as no ignition of the emitted smokes (backside part inner surface self-ignition). This second criteria is here investigated by measuring the part material temperature increase. The Figures 1 and 2 present respectively a picture and an overview of the experimental setup. The composite part is located at 100 mm from the outlet of the cone burner above a vibrating table (sinusoidal vibration of 0.4 mm amplitude and 50 Hz frequency). The oil burner (kerosene-air) operates with a kerosene flow rate of $Q_v^{\text{carb}} = 7.58 \, \text{l/h}$ and the air flow rate is adjusted to $Q_v^{\text{air}} = 25 \, \text{l/s}$ to generate a diffusion flame with: (*i*) Flame temperature of 1100 °C measured at 100 mm and (*ii*) Heat flux of 120 KW/m². The flame temperature is measured at 100 mm by a six thermocouples rack. When the temperature is adjusted and stabilized around 1100 °C the heat flux is measured, thanks to a specific device where water is circulating

along a copper pipe exposed to the flame. The water flow rate and temperature are 226 l/h and 300 K respectively. According to the standards, the minimum temperature increase have to be 5 K. For experimental information, two thermocouples (TC 1 and TC 2) are added and located on the plenum to monitor the internal wall temperatures (cf. Figure 3).Two cameras are also used to record the experimental fire test.
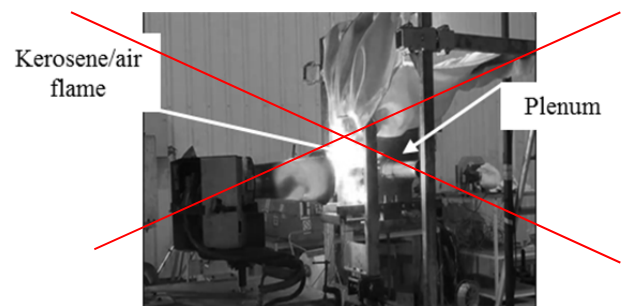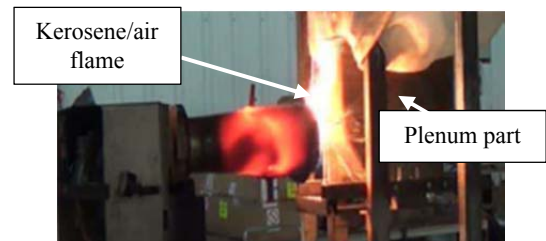

Figure 1 : Photograph of the fire test bench.
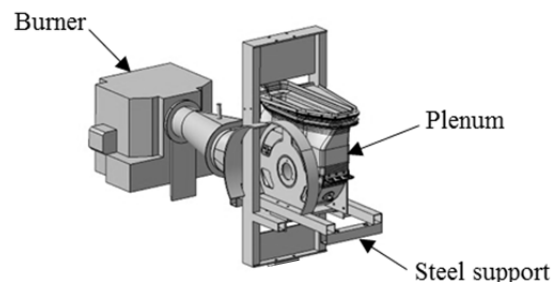
Figure 2: Schematic overview of the experimental setup.

Figure 3: Overview of the TC 1 and TC 2 thermocouple locations.

3. Physical and numerical modelling

3.1. Numerical modelling approach

The present study is based only on the evaluation of the thermal phenomenon, so the flame is modelled with a hot inert gas [3-5]. The hot gas jet is defined by two parameters which are the burner outlet velocity and the flame temperature given above (1100 °C). The fluid

used to model this hot jet corresponds to the combustion products of the diffusion kerosene/air flame for a lean mixture where the global reaction is:
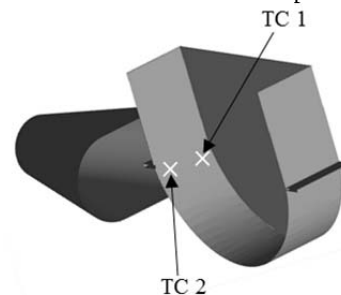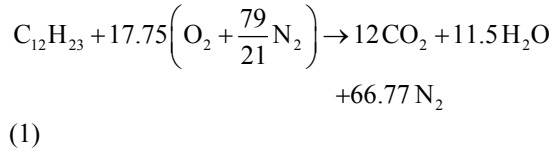
$$C_{12}H_{23} + 17.75\left(O_2 + \frac{79}{21}N_2\right) \rightarrow 12\,CO_2 + 11.5\,H_2O$$
$$+66.77\,N_2$$
(1)

Using equation (1) and the definition of the mass stoichiometric ratio as well as the experimental values of kerosene and air flow rates, the computed value of equivalence ratio is φ=0.88. This equivalence ratio permits to estimate the burner outlet velocity, thanks to a chemical equilibrium calculation performed by the CEA software [6]; its value is equal to 19.5 m/s.

The CFD code employed in this paper solves the three-dimensional time-dependent equations governing fluid motion, and heat transfer. This CFD code uses a finite volume method with the SIMPLE (Semi-Implicit Method for Pressure Linked Equations) algorithm [7] to solve the fluid motion equations. Concerning turbulence treatment, the *k-ε* realizable turbulence model is chosen in this study. This model consists of a new model dissipation rate equation and a new realizable eddy viscosity formulation [8]. The *k-ε* realizable turbulence model has been tested in different benchmark configurations and results show that this model has better performances than the standard *k-ε* model [9-11].

3.2. Numerical calibration of the hot jet

Before studying the temperature evolutions of the plenum exposed to the burner's flame, it is required to perform a preliminary numerical simulation to reproduce the experimental calibration procedure and respect the specifications guideline. The couple of parameters defined in the previous section is used to achieve this numerical calibration. In case the calibration would not be respected, these parameters will have to be adjusted to respect the specified values of the standards. The Figure 4 presents the computational grid of the numerical calibration process which is meshed using an unstructured grids. The outlet region of the model is an environmental pressure boundary (101325 Pa). No-slip adiabatic boundary condition is applied on the burner wall and coupled wall is applied to the copper tube surface.
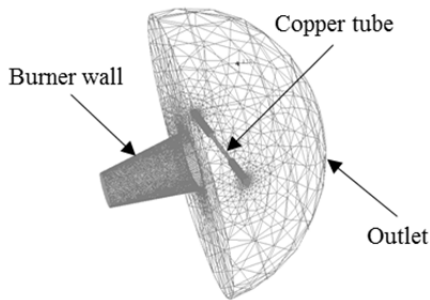
3.3. Thermal properties of the Plenum material

The modelling of the plenum material thermal behaviour needs the utilisation of accurate temperature dependent properties. ~~The~~ A first material studied ~~used~~ in this work is a carbon-phenolic composite which is of interest ~~commonly used~~ in the aerospace industry due to its low thermal conductivity [12-13]. To the best knowledge of the authors, there is no data in the literature on the thermal properties of the studied material. Nevertheless, Engelke et al. [14] gives experimental values of thermal conductivity and specific heat as functions of the temperature for a carbon phenolic material very similar to the one used in this work (i.e. equivalent fibre volume ratio). According to their values, the temperature dependent properties can be given as:

$$C_p = 2\times10^{-5}\,T^3 - 0.0238\,T^2 + 13.128\,T - 1034.8$$
(2)

$$\lambda = -3\times10^{-6}\,T^2 - 0.0031\,T - 0.0049 \tag{3}$$

3.4. Computational domain and conditions

The computational domain considered for this study reproduces the experimental bench presented in the first section. For a second configuration, to study the benefit effect of an air jet at room temperature (300 K) in the internal part of the plenum, an air injector of a 70 mm diameter located at 200 mm above the plenum is added. This distance has been chosen to avoid any perturbation of the flow in this area. Figure 4 illustrates an overview of the burner and the plenum as well as the air injector. In some defined ~~real~~ operating conditions, the APU is flown by air circulation that could decrease the maximum temperature found on the plenum. A numerical study is conducted to evaluate this air circulation impact. To achieve this, three air flow velocities are selected from 0 to 10 m/s. Their values as well as the related flow rates are presented in the Table 1.

Table 1: Jet velocity and flow rate.

Velocity (m/s)	Flow Rate (l/s)
1	3.85
5	19.24
10	38.48

Figure 4: Computational domain for the calibration procedure.
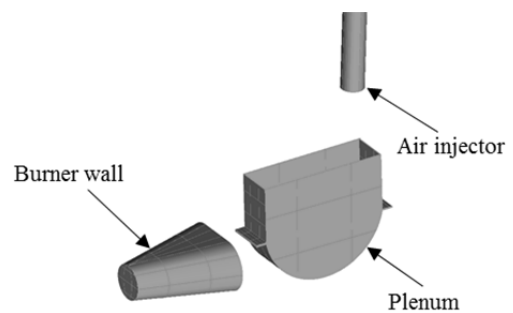

Figure 5 : Overview of the burner, the plenum and the air injector.

The size of the computational domain is a hemisphere with a diameter of 3 m which correspond to ten times the diameter of plenum. A 3,000,000 unstructured mesh is adopted to mesh the plenum and the whole domain (cf. Figure 5).
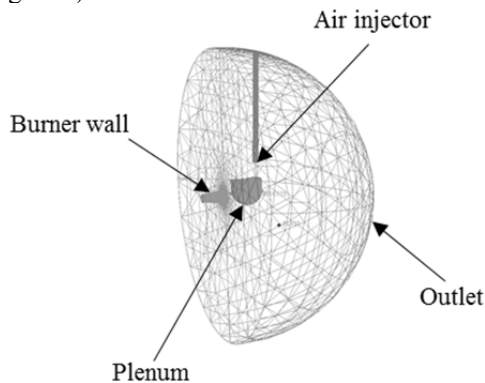

Figure 6: Illustration of the computational grid.

Like the numerical calibration case, the outlet region of the model is the environmental pressure boundary (101325 Pa). A no-slip adiabatic boundary condition is applied on the burner wall and a coupled wall is imposed to the whole plenum geometry. The enhanced wall treatment was used for near-wall modelling. This wall treatment is called the low-Reynolds number approach; it resolves the viscous sublayer and computes the wall shear stress from the local velocity gradient normal to the wall. This wall treatment requires a very fine mesh resolution in wall normal Direction [15]. The y^+ values obtained close to the walls are less than 1, which demonstrates the suitability of the grid used in this paper.

4. Results and discussion

As mentioned in the introduction, the aim of this work is to develop a numerical model of the fire safety tests as an investigation tool for aeronautical certification process. From the velocity and temperature chosen in the previous section (19.5 m/s and 1373 K), it is possible to get the temperature evolution of the water at different times of simulation when regarding the calibration phase. Figure 7 exhibits the numerical evolution of the water temperature as well as the experimental one for this preliminary step of the tests. As one can see from this Figure 7, the computed water temperature is stabilised at 305.9 K after 50 s. The relative gap between the numerical and the experimental temperature elevations do not exceed 1% showing that the criterion imposed by the norms (ISO 2685 and FAA - AC20-135) is valid for the values of velocity and temperature chosen.
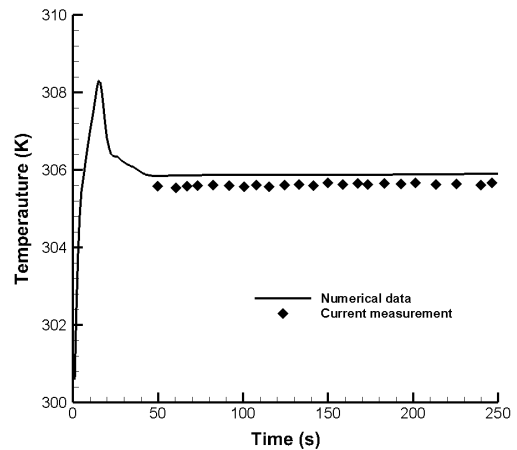

Figure 7: Experimental and numerical water temperature evolutions.

Now regarding the full fireproof test, the temperature evolution of the two thermocouples in the internal surface of the plenum is ~~are~~ compared to the measured values (Figure 8).

It is clear, reading this Figure 8 that the temperatures measured by the two thermocouples on the internal wall of the plenum are very close experimentally (discrepancies lower than 6%). They are also close to the computed values of the thermocouple 2 before 30 s and of the thermocouple 1 after 40 s, not to be unnoticed that the gap between the numerical temperatures increases with the time. The relative error calculated between the experimental and numerical results for the thermocouple 1 is about 19 % whereas the one for thermocouple 2 is around 13 %. These errors could be due to three reasons. First, the approximation on the thermal properties of the carbon-phenolic material used to design the plenum. Indeed, there are no values in the literature on the thermal conductivity and specific heat of the studied material. ~~and the only possibility~~ For this early step of the study, it was therefore decided to use data of a similar material with an equivalent fibre volume fraction. For quantifying the effect of properties, a 50% variation of each physical property was tested. It was found for example that 10% of variation on the specific heat conduct to 10% of variation on the temperature. Second, the simplification of the flame by an inert hot jet which leads to different air temperature fields surrounding the plenum. Indeed, modelling the entire flame will probably show that combustion is not complete at the outlet of the burner and hence it continues near the plenum. Third, the unmodeled thermal degradation of the carbon-phenolic material. Indeed, over 220°C, it was found through some preliminary tests that a mass loss of 1 wt.% is measured. It is expected that over 700°C, the matrix of the composite get completely pyrolysed and/or burned. In spite of these relative errors between experimental and numerical results, the present thermal study gives a first good evaluation of the material temperature and can be used as first indicator in the design process.
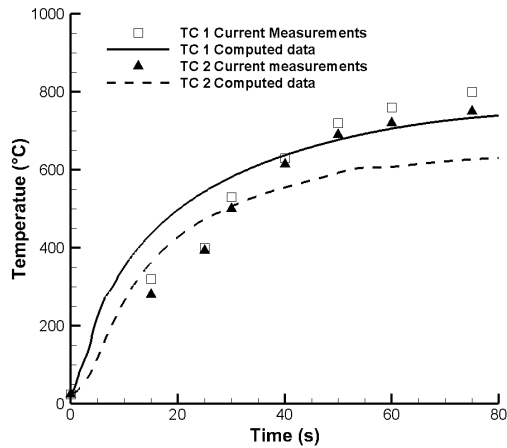
Figure 8: Experimental and numerical temperatures on the internal wall of the heated plenum.

Figure 9: TC 1 temperature evolution in the cooling configuration

Table 2: Effect of the air jet ~~air~~ velocity on TC 1 computed temperature.

Jet velocity (m/s)	Final T (K)	Final T Reduction (%)
0	751	-
1	705	6.1
5	565	24.7
10	465	38.1

In some defined real operating conditions, the APU is flown by air circulation that could decrease the maximum temperature found on the plenum. Thus, it is decided to examine whether an air injection in the internal part of the plenum could have a beneficial effect ~~and hence if certification rules should be adapted in the future~~. Figures 9 and 10 present the computed temperature evolutions of the two thermocouples for different air jet velocities as well as the experimental ones of the ~~thermally protected~~ same studied plenum but equipped with an additional thermal protection. These Figures show the influence of the air jet on the internal temperature approximately after 100 s and both profiles have very different evolutions. Numerical values of TC 1 have a rapid increase before 100 s accompanied by a stabilisation phase during the remaining computational times for different jet air speeds. Compared to numerical data, the experimental temperature of TC 1 exhibits a slower evolution. The increase of this air jet ~~air~~ velocity leads to a decrease of the TC 1 temperature. Before 150 s all computed temperatures of TC 1 are higher than the measured one. After this time, numerical temperatures of TC 1 for air jet velocities of 0 and 1 m/s are higher than experimental data whereas they are lower for 5 and 10 m/s (cf. Figure 8). Table 2 presents the final TC 1 temperatures reached at the stabilisation phase for different velocities and their reduction percentages calculated from the initial case (i.e. without air jet).
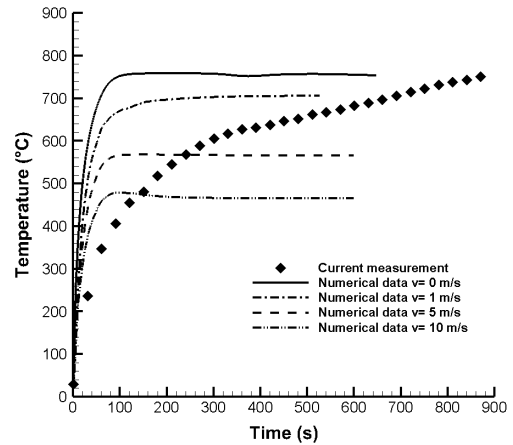
From this Table it can be seen that an increase of the velocity from 1 to 5 m/s induces a final TC1 temperature 1.25 times lower. At the same time an increase of the velocity from 1 to 10 m/s decreases the TC1 temperature by 1.38 times.

Concerning the TC 2 temperature, numerical data show a different behaviour compared to the TC1 temperatures. The evolution can be divided into three phases: a fast increase until 100 s, a decrease between 100 and 300 s and a stabilisation from 300 s till the end of the calculation times. Like the computed TC 1 temperature, the final temperature decrease with the increase of the jet air velocity. However, measured TC 2 temperature present a similar tendency that of TC 1 temperature (cf. Figure 10). Despite the fact that TC1 and TC2 are placed symmetrically for the plenum, a slight temperature shift of about 100 K is found between both because the burner does not impact symmetrically the plenum but it is slightly shifter near TC2. This explains why TC2 receive a higher heat flux from the flame than TC1.
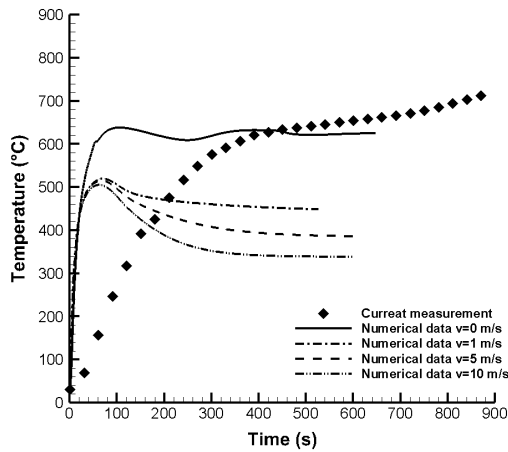
4

Figure 10: TC 2 temperature evolution in the cooling configuration.

Table 3 present the stabilised temperature values and the relative reduction as functions of the jet air velocities. From 1 to 5 m/s, the final computed TC 2 temperature is 1.2 time lower. For an increase of the velocity from 1 to 10 m/s, the computed TC 2 temperature is decreased by 1.3 times.

Table 3: Effect of the jet air velocity on TC 2 computed temperature.

Jet velocity (m/s)	Final T (K)	Final T Reduction (%)
0	624	-
1	448	28.2
5	386	38.1
10	338	45.8

From the above results, it is clear that injecting a defined air flow level ~~an air injection~~ in the internal wall of the plenum ~~seems would facilitate the~~ contributes to lower the part material temperatures (backside part inner surface). This is beneficial to reduce the risk of released smoke and part backside to ignite during the test flame application time, which is a fail criteria for "fireproof" requirement ~~as defined required in the ISO 2685 and FAA AC20-135 standards~~.

5. Conclusion

The numerical study conducted on the thermal behaviour of a composite plenum made of carbon-phenolic material presents a good evaluation of the heating process compared to the experimental measurements performed on a composite part tested according to the AC20-135 and ISO 2685 standards ~~compared to the experimental measurements~~. Also, it has been shown that the air jet in the internal part of the plenum leads to the diminution of the wall temperatures showing its benefit effect. The authors anticipate performing a more reliable analysis with more accurate thermal properties of the studied carbon-phenolic material ~~used to design the plenum~~ as well as additional studies on other materials. To do so, an extensive testing of materials under various stress conditions is expected to get the density, specific heat, thermal conductivity,

emissivity and heat release rate as a function of time and of temperature. A better modelling of the flame (with combustion description) and of the thermal degradation of the carbon-phenolic material (Arrhenius law with release of products and modification of properties) are also expected within the next two years. In future works, a new metrology will be setup on the experimental test bench with possibility of gas sampling for chemical analysis and an in-house heat flux sensor [16] coupled to image processing from previous studies [17]. This metrology will allow a better understanding of the different phenomena and will enable the improvement of the numerical model.

References

1. International Standard. (1998). Aircraft- Environmental Test Procedure for Airborne Equipment-Resistance to Fire in Designated Fire Zones. 2nd ed. ISO 2685
2. US Departement of Transportation. Federal Aviation Administration. (1990). Powerplant installation and propulsion system component fire protection test methods, standards and criteria. AC20-135.
3. Remie, M. J., Cremers, M. F. G., Schreel, K. R. A. M., et al. (2007). Analysis of the heat transfer of an impinging laminar flame jet. International journal of heat and mass transfer, vol. 50, no 13, p. 2816-2827.
4. Remie, M. J., Särner, G., Cremers, M. F. G., Omrane, A., Schreel, K. R. A. M., Aldén, L. E. M., & De Goey, L. P. H. (2008). Heat-transfer distribution for an impinging laminar flame jet to a flat plate. International Journal of Heat and Mass Transfer, 51(11), 3144-3152.
5. Cremers, M. F. G., Remie, M. J., Schreel, K. R. A. M., & de Goey, L. P. H. (2010). Thermochemical heat release of laminar stagnation flames of fuel and oxygen. International Journal of Heat and Mass Transfer, 53(5), 952-961.
6. McBride, B. J., & Gordon, S. (1996). Computer program for calculation of complex chemical equilibrium compositions and applications: II. User's manual and program description. NASA reference publication, 1311, 84-85.
7. Caretto, l. S., Gosman, a. D., Patankar, s. V., et al. (1973). Two calculation procedures for steady, three-dimensional flows with recirculation. In: Proceedings of the third international conference on numerical methods in fluid mechanics. Springer Berlin Heidelberg. p. 60-68.
8. Shih, T. H., Liou, W. W., Shabbir, A., Yang, Z., & Zhu, J. (1995). A new k-ε eddy viscosity model for high Reynolds number turbulent flows. Computers & Fluids, 24(3), 227-238.
9. Suryan, A., Kim, H. D., & Setoguchi, T. (2013). Comparative study of turbulence models performance for refuelling of compressed hydrogen tanks. International Journal of Hydrogen Energy, 38(22), 9562-9569.
10. Chen, A., & Sparrow, E. M. (2009). Turbulence modelling for flow in a distribution manifold. International Journal of Heat and Mass Transfer, 52(5), 1573-1581.
11. Ziani, L., Chaker, A., Chetehouna, K., Malek, A., & Mahmah, B. (2013). Numerical simulations of non-premixed turbulent combustion of CH4–H2 mixtures using the PDF approach. International Journal of Hydrogen Energy, 38(20), 8597-8603.

5

12. Trick, K. A., & Saliba, T. E. (1995). Mechanisms of the pyrolysis of phenolic resin in a carbon/phenolic composite. Carbon, 33(11), 1509-1515.
13. Srikanth, I., Padmavathi, N., Kumar, S., Ghosal, P., Kumar, A., & Subrahmanyam, C. (2013). Mechanical, thermal and ablative properties of zirconia, CNT modified carbon/phenolic composites. Composites Science and Technology, 80, 1-7.
14. Engelke, W. T., Pyron JR, C. M., et Pears, Coultas D. (1967). Thermal and mechanical properties of a nondegraded and thermally degraded phenolic-carbon composite. Southern research inst Birmingham AL.
15. Lateb, M., Masson, C., Stathopoulos, T., & Bédard, C. (2013). Comparison of various types of k–ε models for pollutant emissions around a two-building configuration. Journal of Wind Engineering and Industrial Aerodynamics, 115, 9-21.
16. Chetehouna, K., Séro-Guillaume, O., Sochet, I., & Degiovanni A. (2008) On the experimental determination of flame front positions and of propagation parameters for a fire. International Journal of Thermal Sciences, 47(9), 1148-1157.
17. Rudz, S., Chetehouna, K., & Séro-Guillaume, O. (2011). Metrological Tool for the Characterization of Flame Fronts Based on the Coupling of a Heat Flux Approach with Image Processing Data. Fire technology, 47(2), 491-505.